Available online at www.sciencedirect.com
ScienceDirect
Journal of Photochemistry and Photobiology A: Chemistry 182 (2006) 273–279
Journal of Photochemistry and Photobiology A:Chemistry
www.elsevier.com/locate/jphotochem

Near-IR transient absorption study on ultrafast electron-injection dynamics from a Ru-complex dye into nanocrystalline In_2O_3 thin films: Comparison with SnO_2, ZnO, and TiO_2 films

Akihiro Furube *, Miki Murai, Sadayuki Watanabe, Kohjiro Hara, Ryuzi Katoh, M. Tachiya

National Institute of Advanced Industrial Science and Technology (AIST), Tsukuba Central 5, 1-1-1 Higashi, Tsukuba, Ibaraki 305-8565, Japan

Available online 30 June 2006

Abstract

We investigated the dynamics of photoinduced ultrafast electron injection from the excited state of *cis*-di(thiocyanato)bis(2,2′-bipyridyl-4,4′-dicarboxylate)ruthenium(II) (N3 dye) into the conduction band of nanocrystalline In_2O_3 films by measuring transient absorption of N3-sensitized In_2O_3 films in the wavelength region from 600 nm to 4 μm at 100–250-fs temporal resolutions, and the results were compared with those for N3-sensitized nanocrystalline ZnO, SnO_2, and TiO_2 films. Although the reaction kinetics could not be simply described by a single exponential function and the near-IR transient absorption spectral shapes were dependent on the environmental conditions, the predominant injection time for the In_2O_3 films was 5–10 ps. The SnO_2 and In_2O_3 films showed similar injection dynamics, and the injection times for these films were much shorter than the 150-ps injection time reported for ZnO films. The predominant injection time for the TiO_2 film was within 100 fs, which is in agreement with reported values. The differences in the injection times are qualitatively explained in terms of the density of acceptor states in the conduction bands at the LUMO level of N3 dye.

Keywords: Transient absorption; Electron injection; Ultrafast spectroscopy; Dye-sensitized semiconductor film; In_2O_3

1. Introduction

Metal oxide semiconductor nanocrystalline films coated with dye molecules can be utilized as electrodes in efficient solar cells (Grätzel cells), and basic and applied research aimed at the development of practical applications for these cells has been going on for more than a decade [1,2]. In these cells, injection of an electron from a photoexcited dye molecule chemically anchored on a semiconductor surface into the conduction band of the semiconductor is the first step to produce photocurrent. The rates and yields of interfacial charge separation must be high if a large photocurrent is to be achieved. The charge separation rates can be directly measured by ultrafast spectroscopy with femtosecond time resolution, and many studies aimed at understanding the electron-injection reaction mechanism have been carried out in recent years [3–25].

Choosing a suitable combination of sensitizer dye and semiconductor is important for the high performance of the solar cell device. One of the most promising combinations consists of *cis*-di(thiocyanato)bis(2,2′-bipyridyl-4,4′-dicarboxylate)ruthenium(II) (N3 dye) and titanium dioxide (TiO_2) [26,27], which we call N3/TiO_2 in this paper. The ultrafast electron-injection process has been investigated by many research groups [3,8,9,13,14,28]. The electron-injection time is on the order of a few tens of femtoseconds, and therefore electron injection competes with other relaxation processes within the dye molecule, such as intersystem crossing [29] and intramolecular vibrational relaxation. Ultrafast electron injection is known to be followed by an additional, slower injection in the picosecond time range, and this slow injection accounts for approximately 20% of the total injection yield. This slower injection seems to take place from the relaxed electronic state of N3, that is, the lowest triplet state (T_1). The slow injection has also been interpreted as being due to electron-injection reaction from dye molecules aggregated on the TiO_2 surface [30]. Although the details of the slow injection process have not yet been completely worked out, the main injection reaction clearly occurs within a few tens of femtoseconds in N3/TiO_2.

If we are to understand the electron-injection mechanism in these dye/semiconductor combinations, we must determine

* Corresponding author. Tel.: +81 29 861 2953; fax: +81 29 861 5301.
E-mail address: akihiro-furube@aist.go.jp (A. Furube).

1010-6030/$ – see front matter © 2006 Elsevier B.V. All rights reserved.
doi:10.1016/j.jphotochem.2006.05.026

how the dynamics of ultrafast electron injection depend on the semiconductor. Ultrafast spectroscopy has been used to measure the dynamics of electron injection from photoexcited N3 to several kinds of semiconductors. N3-sensitized ZnO (N3/ZnO) has been studied in several laboratories, including our own, and both ultrafast (<100 fs) and slow (100 ps order) processes occur [22,28,31–34]. Ai et al. measured transient absorption of N3-sensitized SnO_2 and Nb_2O_5 (N3/SnO_2 and N3/Nb_2O_5) and reported a picosecond multiexponential behavior (1–100 ps order), with the behavior depending on the sample preparation and the sample environment [17,18]. In addition, Benkö et al. showed slow electron injection (2.5–50 ps order) in N3/SnO_2 by probing the absorption of oxidized N3 [10].

Because these studies were done under different experimental conditions and thus comparison of the data is difficult, we investigated the electron-injection dynamics in several N3-sensitized semiconductor films of TiO_2, ZnO, SnO_2, and In_2O_3 under identical excitation and environmental conditions. To our knowledge the electron-injection dynamics of N3-sensitized In_2O_3 (N3/In_2O_3) have not been reported with detailed transient absorption spectral data of the reactants and products, although very recently Guo et al. have reported transient absorption kinetics of injected electrons at IR probe wavelengths [36]. Transient absorption spectra in the near-IR region revealed that electronic nature of photoexcited N3 dye was sensitive to the sample environment. We were able to systematically alter the density of acceptor states by changing metal oxide semiconductors. The differences in the injection times could be explained in terms of the density of acceptor states in the conduction bands at the LUMO level of N3.

2. Experimental

2.1. Samples

The procedure for the preparation of dye-sensitized nanocrystalline films has been already reported [28]. For the In_2O_3 film, nanoparticles of In_2O_3 were synthesized by calcination of the corresponding hydroxides, which were precipitated from $In(NO_3)_3$ solutions by adjustment of the solution pH with NH_3. The resulting films had an area of 1 cm^2 (1 cm × 1 cm) and a thickness of 2–5 μm. The sensitizer dye used was *cis*-di(thiocyanato)bis(2,2′-bipyridyl-4,4′-dicarboxylate)ruthenium(II) [Ru(dcbpy)$_2$(NCS)$_2$], generally called N3 dye (Fig. 1). N3 dye was purchased from Solaronix SA and used without purification. For dye sensitization, the nanocrystalline semiconductor films of In_2O_3, SnO_2, ZnO, and TiO_2 were immersed in a solution of dye in 50:50 *tert*-butanol:acetonitrile. For N3/ZnO, the amount of the dye load was kept small to suppress aggregation of the dye molecules [34].

Ground-state absorption spectra of the dyes adsorbed on these films (Fig. 2) were similar to the solution spectra, although the peaks were shifted slightly. The similarity of the spectra suggests that the interaction between the dye and the semiconductor films in the ground state was weak. The N3 dye is known to adsorb strongly on semiconductor surfaces via the carboxyl group(s)

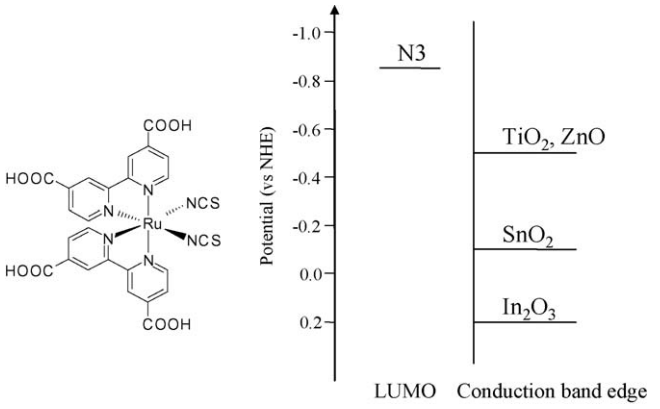

Fig. 1. Molecular structure of N3 and the energy levels of its LUMO and the conduction band edges of the semiconductors investigated in this study.

[27]. The optical transition in the visible region is assigned to the metal-to-ligand charge-transfer (MLCT) transition, which involves electron transfer from the Ru central metal to one of the two bipyridine ligands. The LUMO of N3 is located about 0.35 eV above the conduction band edges of TiO_2 and ZnO and about 1.05 eV above the conduction band edge of In_2O_3 (Fig. 1) [28].

2.2. Femtosecond transient absorption spectroscopy

The details of the femtosecond transient absorption spectrometer have already been described [22–24]. Briefly, the light source for the femtosecond pump–probe transient absorption measurements was a regenerative/multipath double-stage amplifier system consisting of a Ti:sapphire laser (800 nm wavelength, 50 fs FWHM pulse width, 1.4 mJ/pulse intensity, 1 kHz rep-

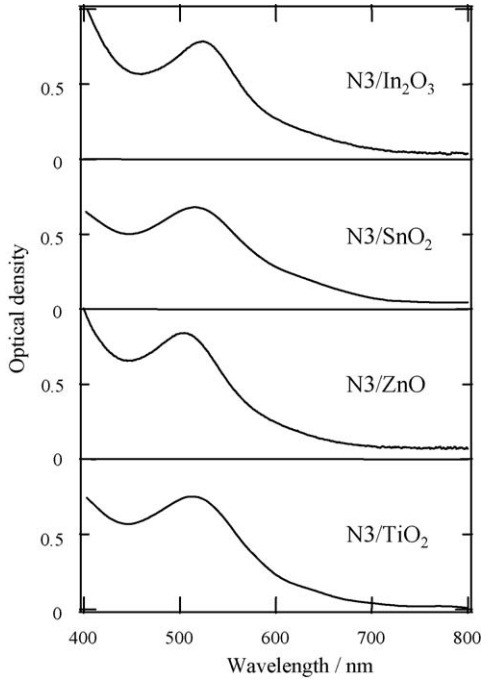

Fig. 2. Ground-state absorption spectra of N3-sensitized semiconductor films.

etition; Spectra Physics, Super Spitfire) combined with two optical parametric amplifiers (OPAs; Spectra Physics, OPA-800). To probe IR wavelengths, another regenerative amplifier system consisting of a Ti:sapphire laser (800 nm wavelength, 160 fs FWHM pulse width, 1.0 mJ/pulse intensity, 1 kHz repetition; Spectra Physics, Hurricane) combined with two OPAs (Quantronix, Topas) was used. For a pump pulse, the output of the OPA at a wavelength of 540 nm with an intensity of several microjoules per pulse at a 500-Hz modulation frequency was used; and for a probe pulse, the output of the other OPA or the white-light continuum generated by focusing the fundamental beam (800 nm) onto a sapphire plate (2 mm thick) was used. The probe beam was focused at the center of the pump beam on the sample, and the transmitted probe beam was then detected by means of a Si, InGaAs, or photoconductive mercury cadmium telluride (MCT) photodetector after passing through a monochromator (Acton Research, SpectraPro-300). The time resolutions of the measurements were about 100 fs in the visible and near-IR regions and about 250 fs at IR wavelengths. All measurements were performed at 295 K.

3. Results and discussion

3.1. Electron-injection dynamics in N3/In_2O_3

Fig. 3a shows the transient absorption spectra of N3/In_2O_3 in the visible and near-IR region (between 600 and 1500 nm) at delay times of 1 and 45 ps. At 1 ps, transient absorption signals were strong in the near-IR region (from 1150 to 1400 nm), whereas those in the visible region (from 700 to 900 nm) were rather weak. In contrast, at 45 ps, the absorptions in the near-IR region and at around 650 nm were weaker than at 1 ps, and the absorption at around 800 nm was stronger.

To analyse the transient absorption spectra of N3/In_2O_3, we obtained reference data by means of nanosecond transient absorption spectroscopy for the same N3/In_2O_3 film and N3 dye in 2:1 solutions of deuterated water and deuterated methanol ($\sim 10^{-4}$ M) at various pH values (Fig. 3b). The number of protons, n, attached to the carboxyl groups of N3 dye was controlled by changing the pH of the solution. Transient absorption spectra of fully protonated ($n=4$), partially protonated ($n=2$), and deprotonated ($n=0$) forms of N3 were measured [35]. The first two spectra ($n=2$ and 4, fully and partially protonated forms) were the same. The excited-state N3 ($N3^*$) in the protonated form absorbed at ~700 and 1400 nm, and $N3^*$ in the deprotonated form absorbed at ~620 and ~1200 nm. Oxidized N3 ($N3^+$) is known to have a peak at 800 nm [3,28]. Its spectrum on In_2O_3 is shown in Fig. 3b. Here, the accompanying absorption band whose intensity increases with wavelength in the near-IR region (over 900 nm) can be assigned to intraband transition of injected electrons in the conduction band of In_2O_3, because this trend is typical for the absorption of electrons in conduction bands [37] and because band-gap excitation of a nanocrystalline In_2O_3 film showed a similar absorption band in the near-IR region (data not shown).

In light of the reference spectra, for the N3/In_2O_3 spectra at 1 and 45 ps, the absorption decays in the near-IR region and at

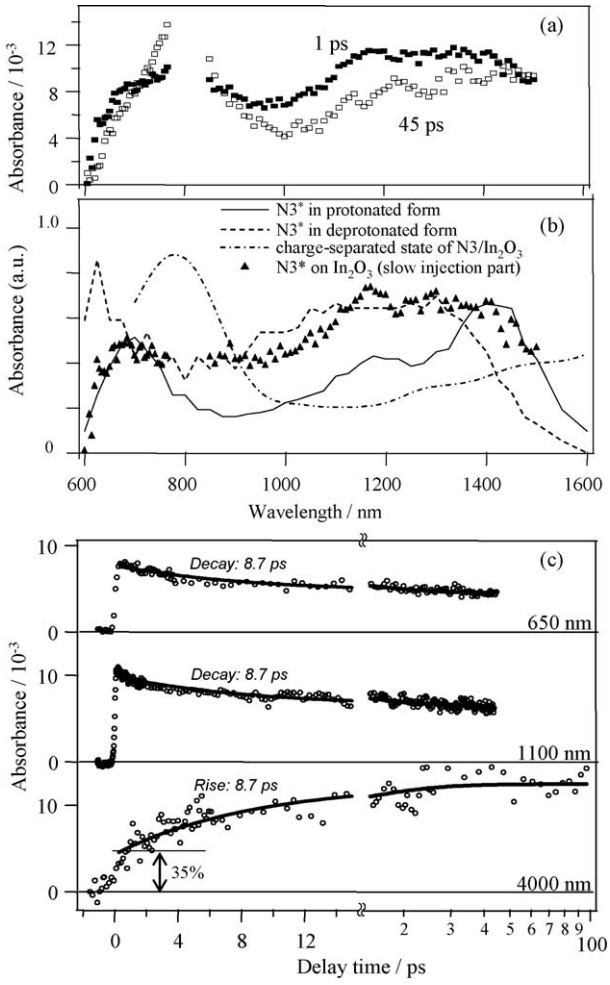

Fig. 3. (a) Transient absorption spectra of N3/In_2O_3 at 1 and 45 ps, (b) transient absorption spectra of $N3^*$ in the protonated and deprotonated forms, the charge-separated state ($N3^+$ on In_2O_3 and injected electrons) at nanoseconds after excitation, and $N3^*$ on In_2O_3 (the contribution of slow injection; see text for details), and (c) temporal profiles of transient absorption of N3/In_2O_3 at probe wavelengths of 650, 1100, and 4000 nm.

~650 nm, whose time profiles are shown in Fig. 3c with single-exponential fitting curves having a decay time of 8.7 ± 0.5 ps and a constant component, can be ascribed to the disappearance of $N3^*$. Moreover, the absorption rise at around 800 nm can be ascribed to generation of $N3^+$. The increase in absorption with wavelength at wavelengths over 1000 nm at 45 ps for N3/In_2O_3 can be ascribed to electrons in the conduction band. That is, the temporal spectral change represents electron injection from $N3^*$ to the In_2O_3 film.

To selectively observe the absorption of injected electrons, we measured the transient absorption time profile at 4000 nm, where electron absorption was very strong (Fig. 3c, bottom panel). The rise curve could be fitted well using a constant of 8.7 ± 0.5 ps, which showed good agreement with the decay constants at 650 and 1100 nm. Additionally, an instantaneous rise component with 35% amplitude relative to the total absorbance was observed clearly, which indicates that there were two pathways for electron injection into the conduction band of In_2O_3. This characteristic is common for electron-injection dynamics

from N3 dye to several kinds of semiconductors, and the faster (<100 fs) process is considered to be electron injection from the unrelaxed state of photoexcited N3, although the detailed mechanism has not been fully clarified [18,38]. Contrastively, a recent study on N3/In_2O_3 by Guo reported absence of instantaneous rise of injected electrons probed between 1880 and 1940 cm^{-1} after 532 nm excitation with a 160 fs time resolution, although the injection dynamics in the picosecond region was roughly the same as ours [36]. The difference between their result and ours for the subpicosecond process is not clear. Our observation of the instantaneous rise component may in part be due to the less time resolution (~250 fs). Different sample preparation methods of In_2O_3 nanocrystalline films may also be responsible.

The presence of the ultrafast pathway indicates that the 1-ps spectrum already includes the contribution of the absorption of $N3^+$ and injected electrons. To obtain the $N3^*$ spectrum due to the slow injection (8.7-ps constant), we subtracted this contribution by using the following equation: Abs(1 ps) − 0.35 × Abs(45 ps) (Fig. 3b, solid triangles). The near-IR absorption band was very broad, and the peak position was hard to discern. The broadness of the band may be due to interaction between $N3^*$ and the In_2O_3 surface, as described for N3/ZnO in our earlier report [22]. We proposed assignment of part of the broad absorption band in the near-IR region to a charge-transfer band in an exciplex between $N3^*$ and some localized surface state on ZnO. The same explanation has been invoked for a system composed of a coumarin-derivative dye (NKX-2311) and ZnO [23]. Other possible origins of the broad absorption band are the coexistence of protonated and deprotonated forms of $N3^*$ and the interaction of $N3^*$ with the neighboring N3 molecules in aggregates composed of dense N3 molecules on the In_2O_3 surface. The latter possibility, however, can be eliminated because we measured the transient absorption spectrum of N3 powder and found that the spectral peak was located at 1500 nm [35].

To change the environment of the N3 dye molecule, we added a single drop of acetonitrile to the N3/In_2O_3 film and measured the transient absorption spectrum at a 1-ps delay time to compare with the spectrum measured in air (Fig. 4a). In the presence of acetonitrile, the absorption band was clearly narrower than that in air, and the band was similar to the absorption band of $N3^*$ in the protonated form (Fig. 3b). Note that the "protonated" form is not in fact the fully protonated form, because at least one carboxyl group must be used to anchor the molecule to the surface. The spectral narrowing may be due to a decrease in the ratio of the deprotonated forms in the presence of acetonitrile.

There are other possible explanations for the spectral narrowing. Acetonitrile molecules around an N3 dye molecule on In_2O_3 may stabilize the dye/surface system by changing, for example, the orientation of the dye with respect to the surface so that the charge-transfer interaction between N3 dye and the surface is suppressed, weakening the charge-transfer band that overlapped the $N3^*$ band. The electron-injection time was slightly shortened, to 5.0 ± 0.5 ps, a value that was obtained from curve fitting for the absorption decay at 1350 nm, as shown in Fig. 4b. The spectral change may have been due to the change in the electronic property of the electron donor, $N3^*$, so that the interaction

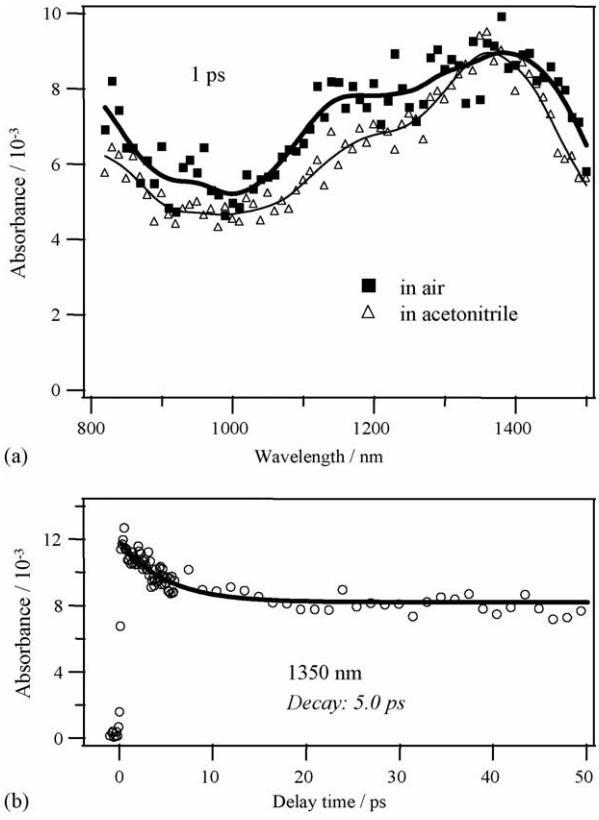

Fig. 4. (a) Transient absorption spectra at 1 ps of the N3/In_2O_3 film in air and covered with acetonitrile and (b) temporal profile of transient absorption of N3/In_2O_3 at 1350 nm.

of $N3^*$ with the surface may have been reduced in acetonitrile. Because $N3^*$ is energetically stabilized by interaction with the surface, the driving force for electron injection is smaller when the interaction of $N3^*$ with the surface is strong.

At present, it is unclear whether the interaction between $N3^*$ and the In_2O_3 surface or the protonation state of $N3^*$ is responsible for the observed broad absorption band of $N3^*$ in the near-IR region. To clarify the origin of this band and its relation to the electron-injection dynamics, further experiments will be necessary. We are planning to perform systematic measurements by controlling the pH of the solution surrounding the dye-sensitized films to investigate the effect of the protonation state of $N3^*$.

3.2. Comparison of In_2O_3, SnO_2, ZnO, and TiO_2

In this section, we discuss differences in the electron-injection dynamics of N3 dye on In_2O_3, SnO_2, and ZnO films, whose conduction bands are mainly composed of the empty s-orbitals of the metal elements (4s for Zn^{2+} and 5s for Sn^{4+} and In^{3+}), and on TiO_2 films, which have a conduction band consisting of empty 3d-orbitals. We have already investigated the charge separation efficiency of these dye-sensitized films by means of nanosecond laser spectroscopy, and we found that the efficiency is almost unity for all the film samples under nanosecond 532-nm laser irradiation [28].

As discussed previously, the ground-state absorption spectra of N3 dye adsorbed on these films were almost identical with

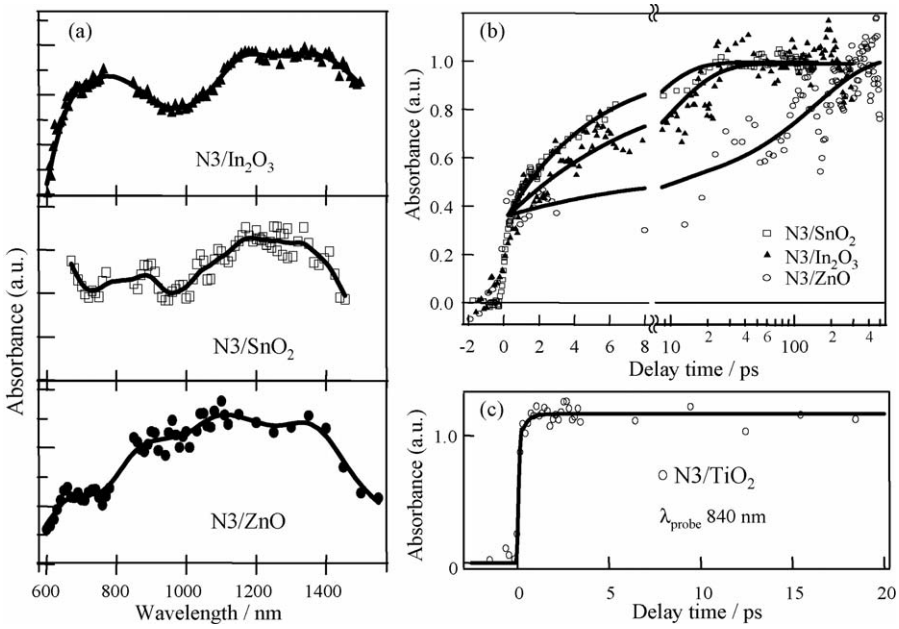

Fig. 5. (a) Transient absorption spectra of $N3/In_2O_3$, $N3/SnO_2$, and N3/ZnO at delay times of 1, 2, and 5 ps, respectively, (b) rise profiles of the transient absorptions at 4000, 1700, and 1960 nm for $N3/In_2O_3$, $N3/SnO_2$, and N3/ZnO, respectively, and (c) transient absorption time profiles at 840 nm for $N3/TiO_2$.

the spectra in solution, indicating that the electronic interaction between the dye and semiconductors in the ground states was weak. In the femtosecond transient absorption experiment, these films were excited at 540 nm. Transient absorption spectra of $N3/In_2O_3$, $N3/SnO_2$, and N3/ZnO are shown in Fig. 5a. The delay times after excitation were set at 1 ps for $N3/In_2O_3$, 2 ps for $N3/SnO_2$, and 5 ps for N3/ZnO to obtain spectra before slow electron injection. Note that in all cases, ultrafast injection within 250 fs was observed as a minor process.

In a previous study of N3/ZnO, we reported a strong transient absorption band ranging between 700 and 1600 nm with a peak at around 1150 nm (Fig. 5a, bottom panel). Because the band was different from the bands of $N3^*$, $N3^+$, or electrons in the conduction band of ZnO, we assigned the band to a charge-transfer absorption of an exciplex formed at the ZnO surface [22]. In the current study, both $N3/In_2O_3$ and $N3/SnO_2$ showed strong, broad near-IR bands similar to the band observed for N3/ZnO, although the band widths were narrower than the width of the N3/ZnO band (Fig. 5a). Because the band width for $N3/In_2O_3$ was affected by the environmental conditions (Fig. 5a) and because the spectrum in the presence of acetonitrile was similar to the transient absorption spectrum of the protonated $N3^*$, we propose that the broadness of these bands is due to interaction between protonated $N3^*$ and the metal oxide surface, or to the contribution of the absorption spectrum of the deprotonated $N3^*$, or both. The broader near-IR absorption band for N3/ZnO may indicate stronger dye–surface interaction than for In_2O_3 and SnO_2, although the nature of the surfaces of these nanocrystalline films is not clear. Alternatively, the N3 molecules may tend to be adsorbed in deprotonated form on ZnO more so than on In_2O_3 and SnO_2.

Because all the samples were measured in air and the excitation wavelengths were identical, we can compare the injection dynamics of the samples. IR wavelengths were utilized for probing the absorption of injected electrons, which allowed us to avoid problems of spectral overlap. These data are shown in Fig. 5b. The probe wavelengths were 4000, 1700, and 1960 nm for $N3/In_2O_3$, $N3/SnO_2$, and N3/ZnO, respectively. The different wavelengths are not a problem for comparing injection dynamics, because the electron absorption bands are very broad and we have shown that there was no difference in the kinetics at different IR wavelengths for a dye-sensitized ZnO film in our earlier report [23]. The results of curve fitting to single or double exponential functions are summarized in Table 1, where injection times and the amplitude ratios of the injection times are listed.

Ultrafast injection within the time resolution of the apparatus, ~250 fs, was observed for all samples, and interestingly the amplitude ratios were almost identical, 34–35% as listed in Table 1. Because the pump wavelength was the same in all the experiments (540 nm), the identical amplitude ratios can be ascribed to electron injection from the unrelaxed state of the excited N3 dye. In the unrelaxed state, that is, in the vibrationally hot S_1 state, electronic coupling between the dye and semiconductors is probably very strong. In a study of photoexcitation of $N3/TiO_2$ with a ~30-fs laser at different excitation wavelengths, faster electron injection is reported to occur when excess vibrational energy is large [8]. Better time resolution is necessary for differentiating the ultrafast injection times within 250 fs. After

Table 1
Parameters for fitting experimental data to single or double exponential functions

	Ultrafast injection, fs (%)	Slow injection, ps (%)
$N3/In_2O_3$	<250 (35)	8.7 (65)
$N3/SnO_2$	<100 (35)	5.0 (65)
N3/ZnO	<100 (34)	6.7 (13)
		150 (53)

thermalization in the excited state, the rise times for electron injection depended on the nature of the semiconductors: the rise times decreased in the order N3/ZnO > N3/In_2O_3 = N3/SnO_2.

In contrast to these samples, whose conduction bands are composed of s-orbitals, N3/TiO_2 showed rapid electron-injection dynamics. We observed the rise profiles of the $N3^+$ band, whose spectral peak is known to be at around 800 nm [3,28]. To avoid spectral overlap with the $N3^*$ band, we measured the transient absorption profile at 840 nm (Fig. 5c). This result for N3/TiO_2 was consistent with the results of previously published studies of N3/TiO_2 [3,8,9,13]. Roughly speaking, in metal oxide materials, the transfer integrals for the d-orbitals of the neighboring metal atoms are smaller than the integrals for s-orbitals. Therefore, the effective mass of the conductive electron is expected to be larger for d-orbital materials. When the effective electron mass is large, the density of states (DOS) near the conduction band edge becomes large. This large DOS for TiO_2 provides a large number of electron acceptor states for electron injection, resulting in fast injection.

Among the s-orbital samples, N3/ZnO showed much slower injection, which may be due to the higher position of its conduction band edge. The DOS, $g(E)$, is related to the effective mass, m^*, by the following equation:

$$g(E) = \frac{\sqrt{2}}{\pi^2\hbar^3} m^{*3/2}\sqrt{E - E_{CB}}, \quad (1)$$

where E_{CB} is the energy of the conduction band edge [38]. The value of m^* for ZnO [39], SnO_2 [40], and In_2O_3 [41,42] is approximately $0.3m_e$, where m_e is the free electron mass. In the case of N3/ZnO, the energy difference from the N3 LUMO to the conduction band edge is smaller than the corresponding energy differences for N3/SnO_2 and N3/In_2O_3 (Fig. 6). Electron injection will occur from the N3 LUMO to its energetically nearby levels in the conduction band. At the N3 LUMO position, the DOS of the ZnO is smaller than that of other materials investigated, and the DOS of SnO_2 seems to be similar to that of In_2O_3. The order of the electron-injection rates and the DOS values at the LUMO level show good agreement. One may think that the broad near-IR absorption band observed in N3/ZnO indicates the strong electronic coupling giving rise to fast electron injection. We think, however, the near-IR absorption represents coupling between $N3^*$ and surface states, and injection rates are determined by coupling between $N3^*$ (strictly speaking, $N3^*$ interacting with surface states) and the bulk conduction band.

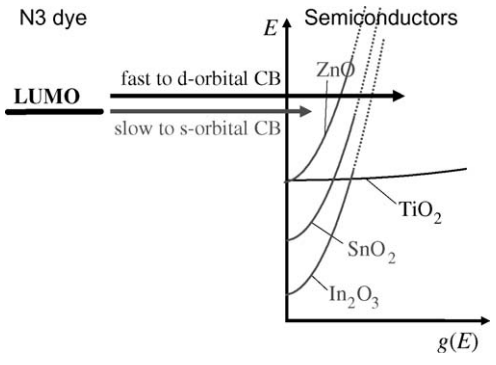

Fig. 6. Energy scheme of electron injection for excited N3 dye on various metal oxide semiconductors: $g(E)$ is the DOS of the conduction band.

Recently, Ai and coworkers reported on an investigation of the dynamics of ultrafast electron injection from N3 to nanoporous Nb_2O_5 thin films by means of femtosecond UV-pump/IR-probe spectroscopy. The conduction band of Nb_2O_5 is mainly composed of empty 4d-orbitals of Nb^{5+}; therefore, rapid injection is expected, owing to the large DOS. However, Ai and coworkers observed slow (~100 ps) injection for the major process as well as a minor < 100 fs process. Because the conduction band edge of Nb_2O_5 is located very close to the LUMO of N3, they attributed the slow process to electron injection into surface defect states energetically below the conduction band edge.

For further understanding of the factors governing the dependence of the electron-injection rate on the semiconductor, experiments that are more controlled will be necessary. For example, to eliminate the effect of surface states below the conduction band, dye molecules having higher LUMO levels would be suitable. N3 dye is an efficient sensitizer for solar cells, but the intramolecular process that occurs after the MLCT photoexcitation is complicated. Intersystem crossing from the singlet excited state to the triplet state occurs in several tens of femtoseconds [8,29], and interligand electron transfer is reported to occur in the picosecond time range [11]. In general, the electron-transfer rate strongly depends on the donor–acceptor distance and the orientation of the donor and the acceptor. Because N3 dye has two bipyridine ligands and adsorption may occur in several modes (via one or two of the four carboxyl groups on a single dye molecule), several types of electron reaction paths should exist from a specific ligand to the conduction band [27]. Organic dye molecules, in which the intersystem crossing time is usually in the nanosecond range, may be appropriate for this purpose.

4. Conclusions

The dynamics of photoinduced ultrafast electron injection from the excited state of *cis*-di(thiocyanato)bis(2,2′-bipyridyl-4,4′-dicarboxylate)ruthenium(II) into the conduction band of a nanocrystalline In_2O_3 film in air were investigated by measurement of transient absorption in the wavelength region from 600 nm to 4 μm at 100–250 fs temporal resolutions. About 35% of the excited N3 molecules underwent rapid electron injection within 250 fs, and the remaining 65% underwent slow injection with a time constant of 8.7 ± 0.5 ps. The two processes are considered to be electron injection from unrelaxed and relaxed states of the excited N3 dye, respectively. The slow injection was affected by the addition of acetonitrile to the film, which led to spectral narrowing of the excited N3 absorption band as well as to a decrease in the injection time. This result indicates that the interaction of excited-state N3 dye with the In_2O_3 surface, or the protonation state of the N3 molecules, or both, influence the electron-injection dynamics. Also, dye aggregation on the In_2O_3 surface was found to be negligible from the observed transient absorption spectral shapes in the near-IR region.

The results for an N3-sensitized nanocrystalline In_2O_3 film were compared with results for N3-sensitized ZnO, SnO_2, and TiO_2 films under identical experimental conditions. Although

the reactions could not be simply described by means of a single exponential function, the dominant injection time for the SnO_2 films was 5 ps, and that for the ZnO film was about 150 ps. The dominant injection time for the TiO_2 film was within 100 fs, as has already been reported. The differences in the injection times could be explained in terms of the density of acceptor states in the conduction bands at the LUMO level of N3 dye. That is, when the acceptor-state density was larger at the LUMO level of N3, faster injection was observed.

Acknowledgements

This work was partially supported by the COE Program (Photoreaction Control and Photofunctional Materials) of the Ministry of Education, Culture, Sports, Science and Technology of Japan (MEXT). A. Furube is grateful to MEXT for a Support of Young Researchers with a Term grant.

References

[1] B. O'Regan, M. Grätzel, Nature 353 (1991) 737–740.
[2] M. Grätzel, Nature 421 (2003) 586–587.
[3] Y. Tachibana, J.E. Moser, M. Grätzel, D.R. Klug, J.R. Durrant, J. Phys. Chem. 100 (1996) 20056–20062.
[4] R. Huber, J.E. Moser, M. Grätzel, J. Wachtveitl, J. Phys. Chem. B 106 (2002) 6494–6499.
[5] Y. Tachibana, S.A. Haque, I.P. Mercer, J.E. Moser, D.R. Klug, J.R. Durrant, J. Phys. Chem. B 105 (2001) 7424–7431.
[6] Y. Tachibana, I.V. Rubtsov, I. Montanari, K. Yoshihara, D.R. Klug, J.R. Durrant, J. Photochem. Photobiol. A Chem. 142 (2001) 215–220.
[7] C. Zimmermann, F. Willig, S. Ramakrishna, B. Burfeindt, B. Pettinger, R. Eichberger, W. Storck, J. Phys. Chem. B 105 (2001) 9245–9253.
[8] G. Benkö, J. Kallioinen, J.E.I. Korppi-Tommola, A.P. Yartsev, V. Sundström, J. Am. Chem. Soc. 124 (2002) 489–493.
[9] J. Kallioinen, G. Benkö, V. Sundström, J.E.I. Korppi-Tommola, A.P. Yartsev, J. Phys. Chem. B 106 (2002) 4396–4404.
[10] G. Benkö, P. Myllyperkio, J. Pan, A.P. Yartsev, V. Sundström, J. Am. Chem. Soc. 125 (2003) 1118–1119.
[11] G. Benkö, J. Kallioinen, P. Myllyperkio, F. Trif, J.E.I. Korppi-Tommola, A.P. Yartsev, V. Sundström, J. Phys. Chem. B 108 (2004) 2862–2867.
[12] R.J. Ellingson, J.B. Asbury, S. Ferrere, H.N. Ghosh, J.R. Sprague, T.Q. Lian, A.J. Nozik, J. Phys. Chem. B 102 (1998) 6455–6458.
[13] J.B. Asbury, R.J. Ellingson, H.N. Ghosh, S. Ferrere, A.J. Nozik, T.Q. Lian, J. Phys. Chem. B 103 (1999) 3110–3119.
[14] R.J. Ellingson, J.B. Asbury, S. Ferrere, H.N. Ghosh, J.R. Sprague, T. Lian, A.J. Nozik, Z. Phys. Chem.-Int. J. Res. Phys. Chem. Chem. Phys. 212 (1999) 77–84.
[15] J.B. Asbury, N.A. Anderson, E.C. Hao, X. Ai, T.Q. Lian, J. Phys. Chem. B 107 (2003) 7376–7386.
[16] N.A. Anderson, T. Lian, Coord. Chem. Rev. 248 (2004) 1231–1246.
[17] X. Ai, J.C. Guo, N.A. Anderson, T.Q. Lian, J. Phys. Chem. B 108 (2004) 12795–12803.
[18] X. Ai, N.A. Anderson, J.C. Guo, T.Q. Lian, J. Phys. Chem. B 109 (2005) 7088–7094.
[19] Y.H. Wang, K. Hang, N.A. Anderson, T.Q. Lian, J. Phys. Chem. B 107 (2003) 9434–9440.
[20] G. Ramakrishna, A.K. Singh, D.K. Palit, H.N. Ghosh, J. Phys. Chem. B 108 (2004) 1701–1707.
[21] S. Iwai, K. Hara, S. Murata, R. Katoh, H. Sugihara, H. Arakawa, J. Chem. Phys. 113 (2000) 3366–3373.
[22] A. Furube, R. Katoh, K. Hara, S. Murata, H. Arakawa, M. Tachiya, J. Phys. Chem. B 107 (2003) 4162–4166.
[23] A. Furube, R. Katoh, T. Yoshihara, K. Hara, S. Murata, H. Arakawa, M. Tachiya, J. Phys. Chem. B 108 (2004) 12583–12592.
[24] A. Furube, R. Katoh, K. Hara, T. Sato, S. Murata, H. Arakawa, M. Tachiya, J. Phys. Chem. B 109 (2005) 16406–16414.
[25] J.F. Xiang, F.S. Rondonuwu, Y. Kakitani, R. Fujii, Y. Watanabe, Y. Koyama, H. Nagae, Y. Yamano, M. Ito, J. Phys. Chem. B 109 (2005) 17066–17077.
[26] M.K. Nazeeruddin, A. Kay, I. Rodicio, R. Humphry-baker, E. Muller, P. Liska, N. Vlachopoulos, M. Grätzel, J. Am. Chem. Soc. 115 (1993) 6382–6390.
[27] M.K. Nazeeruddin, R. Humphry-Baker, P. Liska, M. Grätzel, J. Phys. Chem. B 107 (2003) 8981–8987.
[28] R. Katoh, A. Furube, T. Yoshihara, K. Hara, G. Fujihashi, S. Takano, S. Murata, H. Arakawa, M. Tachiya, J. Phys. Chem. B 108 (2004).
[29] A.C. Bhasikuttan, T. Okada, J. Phys. Chem. B 108 (2004) 12629–12632.
[30] B. Wenger, M. Grätzel, J.E. Moser, J. Am. Chem. Soc. 127 (2005) 12150–12151.
[31] J.B. Asbury, Y.Q. Wang, T.Q. Lian, J. Phys. Chem. B 103 (1999) 6643–6647.
[32] C. Bauer, G. Boschloo, E. Mukhtar, A. Hagfeldt, J. Phys. Chem. B 105 (2001) 5585–5588.
[33] N.A. Anderson, X. Ai, T.Q. Lian, J. Phys. Chem. B 107 (2003) 14414–14421.
[34] H. Horiuchi, R. Katoh, K. Hara, M. Yanagida, S. Murata, H. Arakawa, M. Tachiya, J. Phys. Chem. B 107 (2003) 2570–2574.
[35] M. Murai, A. Furube, M. Yanagida, K. Hara, R. Katoh, Chem. Phys. Lett. 423 (2006) 417–421.
[36] J. Guo, D. Stockwell, X. Ai, C. She, N.A. Anderson, T.Q. Lian, J. Phys. Chem. B 110 (2006) 5238–5244.
[37] J.I. Pankove, Optical Processes in Semiconductor, Dover, New York, 1975.
[38] J.B. Asbury, E. Hao, Y.Q. Wang, H.N. Ghosh, T.Q. Lian, J. Phys. Chem. B 105 (2001) 4545–4557.
[39] B. Enright, D. Fitzmaurice, J. Phys. Chem. 100 (1996) 1027–1035.
[40] G. Sanon, R. Rup, A. Mansingh, Phys. Rev. B 44 (1991) 5672–5680.
[41] I. Hamberg, C.G. Granqvist, K.F. Berggren, B.E. Sernelius, L. Engstrom, Phys. Rev. B 30 (1984) 3240–3249.
[42] H. Odaka, Y. Shigesato, T. Murakami, S. Iwata, Jpn. J. Appl. Phys. Part 1-Regular Pap. Short Notes Rev. Pap. 40 (2001) 3231–3235.